Bull. Soc. géol. Fr., 2004, t. 175, n° 1, pp. 61-72

65 m.y.-long magmatic activity in Sumatra (Indonesia), from Paleocene to Present

HERVÉ BELLON[1*], RENÉ C. MAURY[1], SUTANTO[2], RUBINI SOERIA-ATMADJA[3], JOSEPH COTTEN[1] and MIREILLE POLVÉ[4]

Key words. – Ages (^{40}K-^{40}Ar), Calc-alkaline lavas, Island arc, Sumatra, Java, Indonesia.

Abstract. – Sumatra is the largest volcanic island of the Indonesian archipelago. The oblique subduction of the Indian Ocean lithosphere below the Sundaland margin is responsible for the development of a NW-SE trending volcanic arc, the location of which coincides approximately with the Great Sumatran Fault Zone (GSFZ). We present in this paper ca. 80 new ^{40}K-^{40}Ar ages measured on Cenozoic calc-alkaline to shoshonitic magmatic rocks sampled all along this arc from Aceh to Lampung. The results show that magmatic activity started during the Paleocene (ca. 63 Ma) all along the arc, and was more or less permanent until Present. However, its spatial distribution increased at ca. 20 Ma, a feature possibly connected to the development of the Great Sumatran Fault. The position of Plio-Quaternary magmatic rocks is shifted away from the trench by a few tens of kilometres with respect to that of Paleocene to Miocene ones, a feature consistent with a significant tectonic erosion of the Sundaland margin during the Cenozoic.

The studied samples display typical subduction-related geochemical signatures. However, we have been unable to identify clear geochemical trends, either spatial or temporal. We suggest that the lack of such regular variations reflects a complex igneous petrogenesis during which the contribution of the Sundaland continental crust overprinted those of the mantle wedge and the subducted slab.

65 Ma d'activité magmatique à Sumatra (Indonésie), du Paléocène à l'Actuel

Mots clés. – Ages (^{40}K-^{40}Ar), Laves calco-alcalines, Arc insulaire, Sumatra, Java, Indonésie.

Résumé. – Sumatra, la plus grande île volcanique de l'archipel indonésien, a une forme allongée NW-SE sur 1650 km, parallèlement à la fosse de la Sonde (fig. 1, cartouche). Elle résulte de l'évolution de la marge continentale eurasiatique de la Sonde affectée depuis le début du Cénozoïque par la subduction de la lithosphère océanique indienne. La convergence oblique est en partie accommodée par de grands décrochements, parmi lesquels la Grande Faille de Sumatra (GSFZ) dont le trajet coïncide en de nombreux secteurs avec la position de l'arc volcanique plio-quaternaire.

Nous avons échantillonné les ensembles magmatiques cénozoïques de Sumatra au niveau de 8 secteurs régulièrement répartis le long de l'arc (fig.1 et 2), d'Aceh (1) à Lampung (8). Les analyses géochimiques (éléments majeurs et en traces) de ces roches principalement basaltiques et andésitiques (tabl. I) indiquent leur caractère majoritairement calco-alcalin, faiblement potassique à potassique, ou bien shoshonitique pour quelques échantillons (fig. 3). Ces laves possèdent les caractéristiques minéralogiques et chimiques typiques des magmas d'arc, et présentent notamment des spectres d'éléments incompatibles faiblement à très enrichis (fig. 3) montrant des anomalies négatives en Nb et Ti. On note la présence de magmas dérivés de l'anatexie de la croûte continentale, et généralement mis en place sous forme d'ignimbrites (tuffs de Lampung et de Toba par exemple).

Quatre-vingt datations ^{40}K-^{40}Ar nouvelles de ces roches magmatiques sont présentées en tableau II. Elles démontrent que l'activité magmatique de l'arc de la Sonde a commencé au Paléocène vers 63 Ma, au nord, au centre et au sud de Sumatra (fig. 2), et non à l'Eocène inférieur comme le suggéraient la plupart des travaux antérieurs [Hamilton, 1979]. Ce résultat ne conduit cependant pas à modifier les modèles géodynamiques récents d'évolution du SE asiatique [Rangin *et al.*, 1990a,b ; Hall, 1996, 2002]. Au Miocène terminal, les sites du magmatisme se déplacent de quelques dizaines de kilomètres au plus en s'éloignant de la fosse (fig. 1), ce qui peut refléter l'intervention de processus d'érosion tectonique. A partir de ce stade, l'activité magmatique affecte l'ensemble de l'île, et se localise principalement au niveau de la GSFZ qui semble contrôler souvent sa mise en place.

A l'inverse du cas de l'île voisine de Java (et de nombreux autres arcs insulaires), on n'observe pas à Sumatra de variation régulière des caractéristiques géochimiques des magmas, et en particulier de leur enrichissement en éléments incompatibles, en fonction de leur âge et/ou de leur localisation spatiale (fig. 5). Nous attribuons cette particularité à une histoire pétrogénétique complexe. Au cours de celle-ci, les signatures géochimiques du manteau de l'arc et de la lithosphère subduite ont été en grande partie masquées par l'empreinte laissée par les processus d'anatexie, de contamination par la croûte et d'assimilation couplée à la cristallisation fractionnée.

[1] UMR 6538 Domaines océaniques, IUEM, Université de Bretagne Occidentale, 6 av. Le Gorgeu, CS 93637, 29238 Brest cedex, France.
* Correspondance : bellon@univ-brest.fr.
[2] Jurusan Geologi UPN « Veteran », Jl. Lingkar Utara, 55281 Yogyakarta, Indonesia.
[3] Jurusan Geologi, Institute of Teknology Bandung, Jl. Ganesa, 40132 Bandung, Indonesia.
[4] UMR 5563 LMTG, Université Paul Sabatier, 38 rue des 36 Ponts, 31400 Toulouse, France.
Manuscrit déposé le 18 juillet 2002 ; accepté après révision le 23 juillet 2003.

INTRODUCTION

One of the major features of the Cenozoic geology of Southeast Asia is the prominence of subduction-related magmatism all along the trench-rimmed archipelagoes of Indonesia and the Philippines, staked by hundreds of active/recent volcanoes. Two kinds of magmatic arcs can be distinguished in those areas : (i) long-lived arcs that result from the subduction of major oceanic domains along thousands-km long trenches, which represent major plate boundaries at the global scale, and (ii) generally short-lived arcs that border the quickly evolving boundaries between oceanic and continental microplates/microblocks. A typical example of the former is the northwestern part of the ca. 5,000 km-long Sunda arc, which results from the subduction of the Indian Ocean lithosphere beneath the edge of the Eurasian plate (referred to as the Sundaland) since the early Tertiary. Short-lived (and short) arcs are very common in eastern Indonesia [Sulawesi : Priadi *et al.*, 1994 and Polvé *et al.*, 1997 ; Banda Sea : Honthaas *et al.*, 1998, 1999] and the Philippines. From a petrogenetic point of view, these short arcs are especially useful to document the effects of either abrupt changes in tectonic regime like initiation, end of subduction [Mindanao : Sajona *et al.*, 1993, 1994, 1997] or those of spatially variable compositions of the subducted and/or overriding plates [Luzon arc : Defant *et al.*, 1989, 1990 ; McDermott *et al.*, 1993 ; Maury *et al.*, 1998]. Conversely, long-lived arcs like the Sunda arc are especially good targets to investigate the effects of prolonged and more or less continuous subduction on the composition of the arc mantle wedge through the temporal geochemical variability of the magmas which derive from its melting.

Numerous studies have dealt with the active volcanoes of the northwestern Sunda arc, e.g. the Toba caldera [Chesner and Rose, 1991] and the Ranau one [Bellier *et al.*, 1999] in Sumatra or the Galunggung, Merapi and Bromo in Java. Surprisingly, relatively few data are available concerning the chronology and geochemistry of Tertiary and early Quaternary magmatic rocks in those islands [Hall, 2002]. In Java, an almost continuous magmatic activity is documented from Eocene (ca. 42 Ma) to Present, and its products show a temporal increase in incompatible elements [Bellon *et al.*, 1989 ; Soeria-Atmadja *et al.*, 1988, 1994]. The latter feature suggests that these elements have been transferred from the downgoing oceanic crust to the mantle wedge, and have been accumulated progressively there, because they were relatively slightly tapped by magmatic activity [Juteau and Maury, 1999]. Ocean floor ages identified from magnetic anomalies range from chron MO (120.4 Ma) SE of Sumatra to chron 34 (83.5 Ma) at the western tip of the island ; the younger area except the ridge is between chron 25 (55.9 Ma) and chron 21 (47.9 Ma), according to the digital isochrons by Müller *et al.* [1997].

The purpose of the present study is (i) to demonstrate from a set of ca. 80 new ^{40}K-^{40}Ar ages that magmatic activity occurred almost continuously all along Sumatra since the Paleocene, and (ii) to discuss the origins of the corresponding geochemical variations with regard to the past and present tectonic evolution of this island.

GEOLOGICAL FRAMEWORK

Sumatra is the largest active volcanic island in Indonesia. Roughly 1,700 km long, it trends NW-SW almost parallel to the Sunda Trench (fig. 1 inset), from which it is separated by a ca. 300 km-wide forearc basin including a partly emerged accretionary complex. The present-day subduction vector is oblique (ca. 60° with respect to the trench) and the GPS-measured corresponding convergence rate is 50 mm/year [Chamot-Rooke and Le Pichon, 1999 ; Michel *et al.*, 2001]. The subducted Indian Ocean lithosphere has been tomographically imaged down to depths of at least 1,500 km, and the downgoing slab is teared beneath central/northern Sumatra [Widiyantoro and van der Hilst, 1996]. The oblique convergence is partly accommodated by two major strike-and-slip faults : the Great Sumatran Fault Zone (GSFZ ; also referred to as the Semangko Fault) onland and the Mentawai Fault in the forearc region [Diament *et al.*, 1992 ; Malod and Kemal, 1996]. This mechanism is extensively described by Bellier *et al.* [1999]. The ages of the subducting oceanic crust range from late Cretaceous in front of the southern part of Sumatra, east of the fossil aseismic Investigator ridge, to Paleocene then Eocene northeastwards. The Wharton fossil ridge enters the trench in front of Central Sumatra (fig. 1 inset). Terrigenous sediments from the Nicobar submarine fan, the source of which was the Irrawaddy river, are abundant off northern Sumatra [Davies *et al.*, 1995].

The thickness of the Sumatra crust is ca. 30 km, a typical continental value [Kopp *et al.*, 2001]. Most of the island is geologically a part of the Sundaland [Simandjuntak and Barber, 1996], a set of Gondwana fragments dating from the Permo-Carboniferous, to which were accreted a number of terranes during the Mesozoic [McCarthy *et al.*, 2001]. For instance, in central and southern Sumatra (inset fig. 1), the Mergui microplate is made of Upper Paleozoic Gondwana formations juxtaposed to the oceanic (island-arc related) Woyla terrane along the Lematang suture zone [Cameron *et al.*, 1980 ; Pulunggono and Cameron, 1984]. The Paleozoic and Mesozoic formations are crosscut by a number of subduction-related granitoids ranging in age from Permian to early Cretaceous [McCourt *et al.*, 1996]. Those located east of the GSFZ are highly radiogenic in Sr and share many geochemical characteristics with S-type granites from Thailand, Burma and Malaysia, while those outcropping west of the GSFZ are island arc-related, and display Sr isotopic ratios lower than 0.706 [Gasparon and Varne, 1995].

Cenozoic magmatic rocks overlie and/or crosscut these Paleozoic and Mesozoic units. They trend NW-SE all along the island, near or west of the Great Sumatran Fault Zone (fig. 1 inset). The location of many Quaternary/active volcanoes is controlled by this major strike-and-slip fault : large collapse calderas, e.g. those of lake Toba and lake Ranau, are limited by the bounding faults of pull-apart basins located along, or parallel to, the Great Sumatran Fault [Bellier and Sébrier, 1994 ; Bellier *et al.*, 1999]. Cenozoic magmatic activity is considered to have started at ca. 60 Ma [McCourt *et al.*, 1996], and developed during the early Miocene (20 Ma) when the Sumatran Fault became active [McCarthy and Elders, 1997].

Exposures of magmatic units are generally poor in western Sumatra, due to the dense Equatorial forests and lateritic alteration profiles. Three field trips conducted from

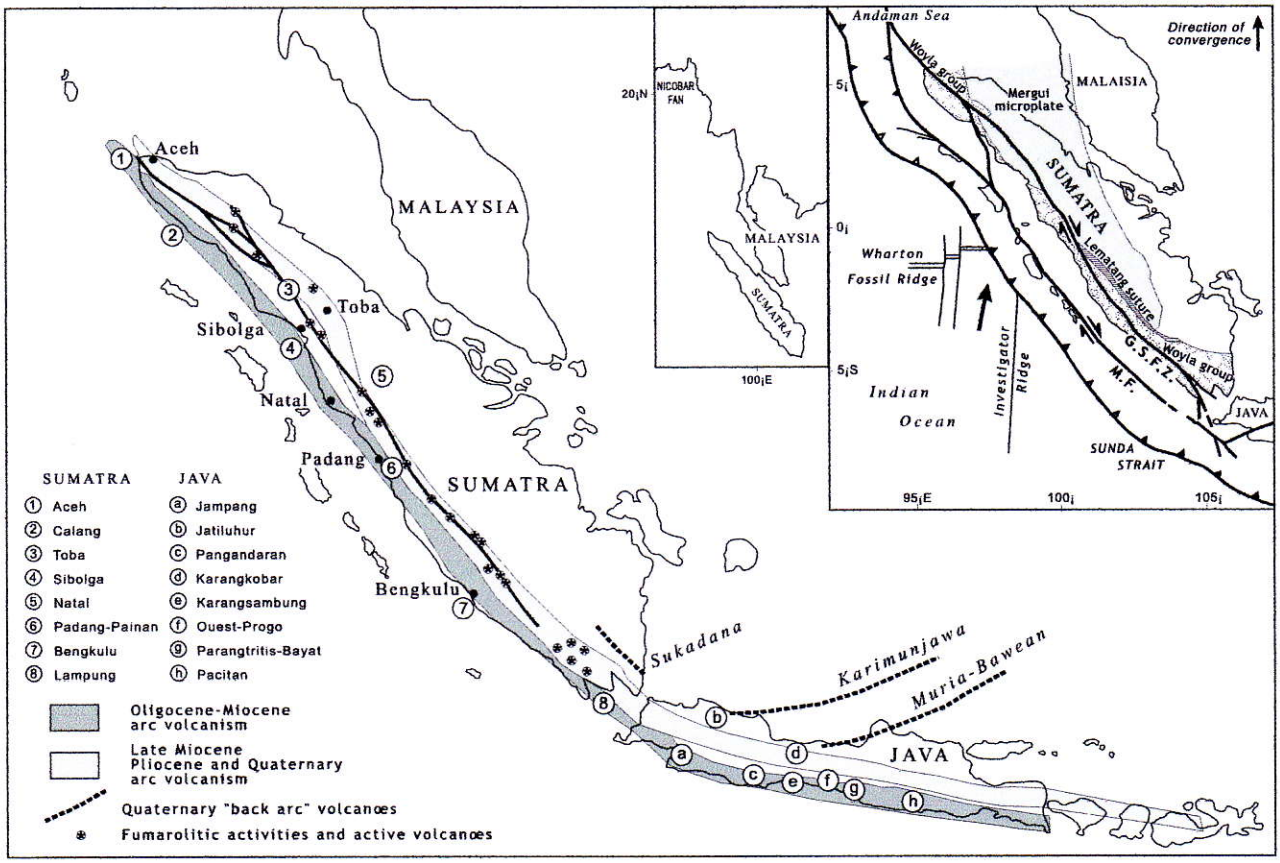

FIG. 1. – Schematic map of Sumatra and Java showing the eight sectors (numbers 1 to 8) in which Cenozoic magmatism in Sumatra has been investigated and the temporal change of the location of the Sunda magmatic arc. Inset shows the main tectonic patterns of Sumatra together with some geological features quoted in the text : GSFZ : Great Sumatran Fault Zone ; MF : Mentawai Fault ; WFR : Wharton Fossil Ridge ; IR : Investigator Ridge and. Convergence vector according to Tregoning *et al.* [1994].

FIG. 1. – *Carte schématique de Sumatra et Java présentant les 8 secteurs d'étude du magmatisme cénozoïque de Sumatra (numéros1 à 8) ainsi que l'évolution de la position de l'arc magmatique de la Sonde au cours du Cénozoïque. En cartouche sont représentés les principaux traits structuraux de Sumatra ainsi que divers éléments géologiques mentionnés dans le texte. GSFZ : zone de la grande faille de Sumatra ; MF : zone de faille de Mentawai ; WFR : ride fossile de Wharton ; IR : ride Investigator. Direction de convergence selon Tregoning* et al. *[1994].*

1993 to 1995 allowed us to sample eight areas labelled 1 (Aceh) to 8 (Lampung) from NW to SE. In most of them, we found a wide range of $^{40}K/^{40}Ar$ ages from Paleocene-Eocene to Plio-Quaternary (fig. 2). Sampling was usually made along roads or rivers, and although we collected ca. 250 fresh or relatively fresh rocks. We are fully aware that this set is far from being exhaustive or simply representative. In particular, we were unable to sample a number of densely forested mountain areas of uneasy access.

ANALYTICAL METHODS

Major and trace element data were obtained by Inductively Coupled Plasma-Atomic Emission Spectrometry (ICP-AES). The samples were finely powdered in an agate grinder. International standards were used for calibration tests (ACE, BEN, JB-2, PM-S and WS-E). Rb was measured by flame emission spectroscopy. Relative standard deviations are ±1 % for SiO_2 and ± 2 % other major elements except P_2O_5 and MnO (± 0.01 %), and ca. 5 % for trace elements. The analytical techniques are described in Cotten *et al.* [1995]. The corresponding chemical analyses are listed in table I.

^{40}K-^{40}Ar datings were performed on whole-rock samples, with the exception of separated feldspars and biotites from rhyolites PR 71 (sector 3) and R1 (sector 8) (table II). After crushing and sieving, the rock fraction of 0.3 to 0.15 mm in size was cleaned with distilled water and then retained for analytical purposes : (i) one aliquot was powdered in an agate grinder for K analysis by atomic absorption after HF chemical attack, and (ii) 0.3 to 0.15 mm grains were used for argon isotopic analysis. Argon extraction was performed under high vacuum by induction heating of a molybdenum crucible. Extracted gases were cleaned on two titanium spunge furnaces and finally purified by using two Al-Zr SAES getters. Isotopic composition of argon and concentration of radiogenic ^{40}Ar were measured using a 180°-geometry stainless steel mass spectrometer equipped with a 642 Keithley amplifier. The isotopic dilution method was applied using a ^{38}Ar spike buried as ions in aluminium targets following the procedure described by Bellon *et al.*

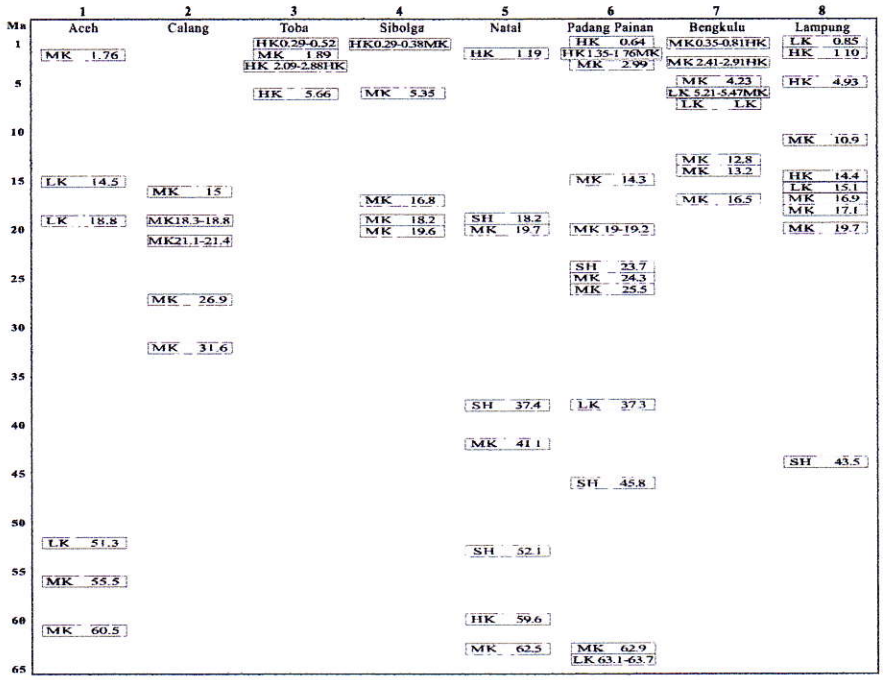

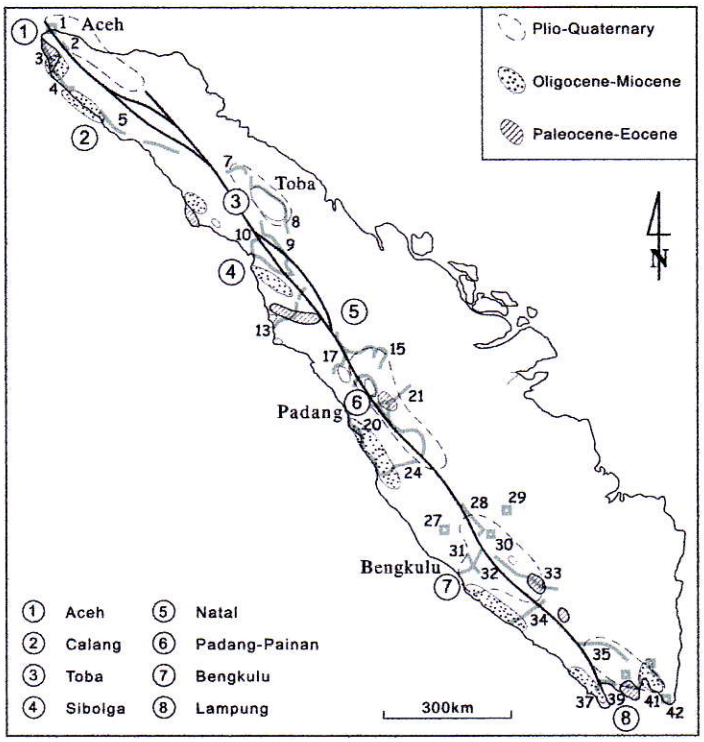

FIG. 2. – Spatial and temporal distribution of Cenozoic magmatism in Sumatra and position of the sampling areas (circled numbers) discussed in this study : 1 : Aceh ; 2 : Calang ; 3 : Toba ; 4 : Sibolga ; 5 : Natal ; 6 : Padang-Painan ; 7 : Bengkulu ; 8 : Lampung. Heavy lines show our main sampling cross-sections, labelled from 1 to 42. Detailed sampling maps can be found in Sutanto [1997] and are available on request to the authors. Cross-sections referred to in tables I and II are : 1 ; 2 ; 3 ; 4 ; 5 ; 7 ; 8 ; 9 ; 13 ; 15 ; 17 ; 20 ; 21 ; 23 ; 24 ; 27 ; 28 ; 29 ; 30 ; 31 ; 32 ; 33 ; 34 ; 35 ; 37 ; 39 ; 40 ; 41 ; 42. Abbreviations for magmatic types are. B : basalts ; BA : basaltic andesites ; A : andesites ; D : dacites ; R : rhyolites ; LK : low-K calc-alkaline ; MK : medium-K calc-alkaline ; HK : high-K calc-alkaline ; SH : shoshonitic ; UK : ultrapotassic. Ages are given in Ma.

FIG. 2. – *Distribution spatio-temporelle du magmatisme cénozoïque de Sumatra et position des secteurs d'échantillonnage de cette étude (les coupes principales sont indiquées en trait gras). Les cartes détaillées de position des échantillons étudiés sont données par Sutanto [1997] et peuvent être communiquées sur demande auprès des auteurs. Abréviations des types magmatiques : B : basaltes ; BA : andésites basaltiques ; A : andésites ; D : dacites ; R : rhyolites ; LK : laves calco-alcalines faiblement potassiques ; MK : laves calco-alcalines moyennement potassiques ; HK : laves calco-alcalins fortement potassiques ; SH : laves shoshonitiques ; UK : laves ultrapotassiques. Les âges sont donnés en Ma.*

TABLE I. – Geochemical analyses of selected lavas from Sumatra (oxide weight % for major elements, ppm for trace elements). Sampling areas and cross-section numbers corresponding to analysed samples are given in table II and are shown in figure 1 caption.
TABL. I. – *Analyses géochimiques (% pondéral d'oxydes pour les éléments majeurs, ppm pour les éléments en trace) de laves de Sumatra. La correspondance des codes des échantillons analysés avec la numérotation des régions d'échantillonnage et des coupes est donnée dans le tableau II. Les zones d'échantillonnage et des coupes sont présentées en figure 1 et dans sa légende.*

	Paleocene, Eocene and Oligocene volcanism										Miocene volcanism								Pliocene and Quaternary volcanism							
	LM 118	NL 40	NL 41	LM 124	SU 49	LM 116A	NL 36	NL 37	TT 148	TP 33	PN 26	CL 140	IP 113	GB 15	SB 83	NL 34	CL 131	MN116	PR 61	BR 104	PR101B	UB 110	PR 71	SR 53	SB 82	SM 76
Age (Ma)	63.1	62.5	59.6	55.5	52.1	51.3	41.1	37.4	31.6	25.5	23.7	21.4	18.8	18.7	16.8	18.2	15.0	13.2	5.70	2.10	1.90	1.76	0.60	0.33	0.29	0.12
wt %																										
SiO_2	49.3	45.8	57.4	48	48	45.6	58	47	53.4	65	49.4	49.7	52	60.6	59.2	48.25	53.6	58.5	63.25	58	52.5	57.6	68.45	58.2	51.9	59.8
TiO_2	0.95	0.93	0.76	1.06	0.79	1.24	0.63	0.98	0.96	0.29	0.81	0.86	0.67	0.62	0.6	0.87	0.65	0.92	0.56	0.78	1.13	0.7	0.44	0.79	0.89	0.66
Al_2O_3	14.05	14.1	17.55	15.1	16.55	18.1	17.9	14.8	17	15.5	19.15	19.7	19.25	16.1	17.35	15.35	17.68	17.65	16.35	17.58	18.45	17.9	14.83	16.8	20.7	17.1
$Fe_2O_3^*$	11	12.9	7.01	13.4	10.65	13	6.92	12.37	8.37	3.27	10.5	8.96	8.08	5.55	6.18	11.28	7.6	6.70	5.42	7.96	10	7.65	3.78	7.35	8.94	7.14
MnO	0.18	0.2	0.21	0.17	0.22	0.2	0.13	0.2	0.16	0.25	0.2	0.16	0.17	0.09	0.15	0.18	0.12	0.16	0.12	0.19	0.17	0.15	0.08	0.17	0.16	0.15
MgO	8.3	7.85	2.65	6.26	4.96	8	3.09	6.47	4.89	0.58	4.75	4.81	3.87	3.2	3.39	6.28	4	2.80	1.98	3.01	3.85	3.09	1.06	3.32	3.32	3.05
CaO	8.65	11.25	3.5	7.75	10.45	6.95	6.7	9.6	8.58	4.8	8.3	10.2	8.9	5.1	6.3	9.85	6.79	5.90	5.35	7.67	7.8	7.4	3	7.3	9.65	6.55
Na_2O	3.85	2.64	4.11	3.92	3.05	2.65	3.29	2.85	3.37	5.42	3.79	3.06	4.85	3.55	3.32	3.25	3.25	3.85	2.22	2.65	2.42	3.45	3.04	2.94	2.96	2.91
K_2O	0.72	1.22	3.23	0.76	2.17	0.3	1.06	2.33	0.66	1.13	2.28	0.57	0.25	2.09	1.39	1.97	0.78	1.38	2.75	1.99	1.24	1.37	2.89	2.34	0.78	1.92
P_2O_5	0.25	0.29	0.33	0.29	0.42	0.31	0.18	0.33	0.17	0.16	0.33	0.15	0.34	0.13	0.12	0.33	0.22	0.24	0.14	0.21	0.27	0.18	0.01	0.17	0.19	0.14
LOI	2.64	2.69	2.82	2.83	2.58	3.16	2.46	2.56	2.11	3.5	0.72	1.7	1.34	3.11	1.54	2.59	2.74	1.97	1.48	0.38	1.93	0.58	2.82	0.76	0.39	0.08
TOTAL	99.89	99.87	99.57	99.54	99.94	99.41	100.36	99.76	99.67	99.9	100.23	99.87	99.74	100.14	99.54	100.2	98.13	100.07	99.62	100.42	99.76	100.07	100.4	100.14	99.88	99.5
ppm																										
Rb	12	19.2	62	13	36	6	44	33.5	23	16.8	58	10	6	74	39	30.5	15	29.5	9	67	64	36	133	80	19.5	63
Ba	108	300	520	167	575	38	205	533	160	338	450	126	64	295	242	417	195	212	714	560	36	313	690	395	195	344
Nb	2.4	1.3	2.1	2.5	2.9	3.6	3.1	1.5	2.8	4.4	2.1	1.4	1.7	4	2.5	1.8	2.5	5.4	9.6	8	11.4	3.9	204	7.7	4	4.8
La	17	9.4	16	9.9	16.2	12.6	11.2	11.6	7.4	19.5	13.1	7	12	12	11.2	11.5	10.5	17	34	30.5	32	28	47	26.5	13.2	19
Ce	41	24	33	27.5	38	32	27	28.5	18.5	52	27	17.5	29	3	24	26.5	25.5	36	6	62	72	59	13.7	57	29	42
Sr	630	615	690	930	855	260	420	546	270	342	944	331	1620	192	248	588	379	276	235	460	475	380	84	284	355	328
Nd	78	16	23.5	18.5	24	22	14.5	19.5	11.5	22	16.5	11.8	19	17	13	19.5	15.5	21	25	27	36	34	31.5	28	16	20
Zr	30	53	97	66	68	76	74	76	84	39	24	66	42	136	116	72	89	84	22	87	164	118	38	208	106	133
Eu	1.75	1.25	1.68	1.3	1.6	1.3	0.93	1.4	1.01	1.05	1.15	0.94	1.26	0.84	0.84	1.39	1.04	1.23	1.04	1.28	1.69	2.1	1.1	1.18	1.14	1.01
Dy	4.15	3.8	4.7	3.9	4.4	4.8	3.9	4.1	4.2	2.8	2.9	3.8	3.5	5.2	4	4	3.5	5.1	3.8	4.3	5.6	8.3	24.5	5.4	4.2	4.2
Y	21	21	27	22.5	24	27	25.5	23	27	16	17	23	20.5	32.5	27	22	22	30	23.5	26.5	31	54	3.8	34.5	26	26.5
Er	2.1	1.9	2.7	2.1	2.2	2.7	2.3	2.2	2.5	1.6	1.6	2.2	2	3.2	2.6	2	2	3.1	2.2	2.6	2.9	5.5	2.5	28	2.5	2.8
Yb	1.78	1.85	2.3	1.95	2.15	2.4	2.34	1.94	2.57	1.27	1.42	2.37	1.82	3.13	2.65	1.9	2.05	2.78	1.96	2.52	2.7	5.4	2.32	2.7	2.54	2.6
Cr	235	50	10	52	10	77	9	75	118	3	8	34	12	52	3	70	18	22	6	6	26	8	6	20	8	11
Ni	52	48	5	27	15	40	5	30	33	2	15	18	18	24	12	29	9	7	2	3	4	7	4	6	12	4
Co	38	47	15	47	34	44	19	38	26	2	29	25	21	16	17	37	20	13	1	18	18	19	6	19	25	18
Sc	36.5	40	14	30	26	33	17.3	36	31	2.8	26	28	20	18.3	2	34.5	16	22	13	17.5	19.3	17	8.9	26.5	25	21
V	266	345	141	370	320	360	160	325	250	8	304	256	245	138	16	320	172	156	105	195	178	192	42	187	242	172

[1981]. Ages listed with their respective characteristic parameters in table II, are calculated using the constants recommended by Steiger and Jäger [1977] and ± 1σ errors are calculated following the equation of Mahood and Drake [1982].

GEOCHEMICAL DATA

Major elements and petrographic types

Representative major and trace element analyses of Cenozoic magmatic rocks of Sumatra are given in table I. Plutonic rocks range in composition from rare gabbros to dominant granites through moderate amounts of diorites and granodiorites. In a K_2O/SiO_2 diagram most of them (with the exception of two low-K samples from Padang) plot within the fields of moderately potassic (medium-K) to highly potassic (high-K) calc-alkaline magma series. They contain quartz, potassic feldspar, plagioclase, Fe-Ti oxides and biotite. Additional amphibole is common, especially in the granodiorites. Additional petrographic data can be found in Sutanto [1997].

Volcanic rocks range in composition from very common basalts, basaltic andesites and andesites to rare dacites and moderate amounts of rhyolites. Most of them plot in the medium-K or high-K calc-alkaline fields, and their pattern in figure 3 matches approximatively that of the less abundant plutonic rocks. Low-K calc-alkaline and shoshonitic lavas are less abundant (fig. 3 and table II). The silica and potassium contents of the lavas are apparently not linked to their geographic position (areas 1 to 8). For instance, Quaternary rhyolitic tuffs occur in northern (Toba, 3), central (Padang,

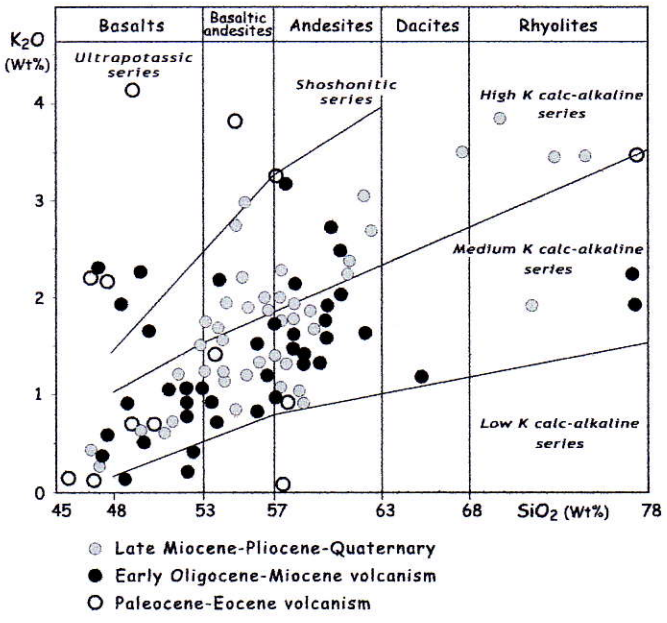

FIG. 3. – K_2O-SiO_2 plot and classification of Sumatra lavas. Petrographic types and series are determined according to Peccerillo and Taylor's [1976] classification slightly modified according to Maury [1984]. B : basalts ; BA : basaltic andesites ; A : andesites ; D : dacites ; R : rhyolites ; LK : low-K calc-alkaline ; MK : medium-K calc-alkaline ; HK : high-K calc-alkaline ; SH : shoshonitic ; UK : ultrapotassic.
FIG. 3. – *Classification des laves de Sumatra à l'aide du diagramme K_2O-SiO_2 de Peccerillo et Taylor [1976] légèrement modifié selon Maury [1984]. B : basaltes ; BA : andésites basaltiques ; A : andésites ; D : dacites ; R : rhyolites ; LK : laves calco-alcalines faiblement potassiques ; MK : laves calco-alcalines moyennement potassiques ; HK : laves calco-alcalines fortement potassiques ; SH : laves shoshonitiques ; UK : laves ultrapotassiques.*

TABLE II. – Isotopic ^{40}K-^{40}Ar datings of samples from Sumatra. Ages with errors at one sigma level are calculated with Steiger and Jäger [1977] constants. Results are the average of two radiogenic argon (Ar*) analyses. Sampling areas and cross-section numbers are shown in figure 1 and 2 ; f : flow ; d : dyke ; t : ignimbritic tuff ; LK : low-K calc-alkaline ; MK : medium-K calc-alkaline ; HK : high-K calc-alkaline ; SH : shoshonitic.

Center	Sample and outcrop		Type and parentage		Age (Ma)	±	error 1sigma	K_2O (wt%)	$^{40}Ar_R$ $10^{-7}cm^3.g^{-1}$	$^{40}Ar_R$ (%)	^{36}Ar $10^{-9}cm^3.g^{-1}$	LOI (wt%)	Analysis number	C.S. number
1	UB 110	f	Andesite	MK	1.76	±	0.06	1.41	0.8	26.7	0.74	0.58	B 3778-4	1
	LM 126	d	Basalt	LK	14.5	±	1.17	0.21	1 25	13.3	2.78	6.86	B 3740-2	3
	IP 113	f	Basalt	LK	18.8	±	0.49	0.32	1.91	46.9	0.73	1.34	B 3747-9	2
	LM 116A	t	Basalt	LK	51.3	±	1.5	0.31	5.2	35.2	2.24	3.16	B 3758-2	3
	LM 124	d	Basalt	MK	55.5	±	1.5	0.78	14.08	70.6	1.98	2.83	B 3759-3	"
	LM 118	f	Basalt	MK	57.9	±	1.4	0.8	16.6	54.	4.88	2.64	B 4213-2	"
					63.1	±	1.5	0.8	18.2	83.5	1.37	2.64	B 4219-8	"
2	CL 131	d	Bas. andesite	MK	15.0	±	0.38	0.91	4.39	52.3	1.35	2.74	B 3736-6	4
	CL 136	d	Andesite	MK	17.5	±	0.42	1.40	7.92	59.3	1.83	2.14	B 3751-4	"
	CL 132	d	Andesite	MK	18.3	±	0.44	1.31	7 76	62.1	1.59	2.42	B 3753-6	"
	GB 15	d	Andesite	MK	18.7	±	0.44	2.07	12.54	74.	1.49	3.11	B 3544-6	"
	CL 135 B	d	Basalt	MK	18.8	±	0.59	0.80	4.87	31.5	3.59	2.31	B 3801-3	"
	CL 141 A	f	Basalt	MK	18.8	±	0.45	1.23	7.47	67 7	1.21	1.30	B 3737-7	"
	CL 135 C	d	Andesite	MK	21.1	±	0.60	1.47	10.08	37.9	5.59	1.43	B 3752-5	"
	CL 140	f	Basalt	MK	21.4	±	0.59	0.60	4.16	40.9	2.04	1.70	B 3798-9	"
	TT 144	d	Basalt	MK	26.9	±	0.72	0.63	5.49	43.2	2.45	4.03	B 3760-4	5
	TT 148	d	Bas. andesite	MK	31.6	±	0.85	0.90	9.18	42.3	4.24	2.11	B 3750-3	"
3	BR 107	f	Andesite	MK	0.48	±	0.11	2.53	0.39	3.7	3.47	1.29	B 3827-3	7
	PR 98A	f	Bas. And.	MK	0.52	±	0.03	1.91	0.32	13.5	0.69	0.45	B 3789-8	"
	PR 71	t	Rhyolite	HK	0.63	±	0.05	3.47	0.7	9.4	2.28	2.82	B 4097-8	8
	(fds)				0.38	±	0.06		0.45	4.8	3.05		B 4481-7	
	(bio)				1.81	±	0.14	3.39	1.97	10.5	5.7		B 4095-6	
	PR 101B	dl	Basalt	MK	1 89	±	0.23	1.47	0.92	6.9	4.11	1.93	B 3946-9	8
	BR 104	f	Andesite	HK	2.09	±	0.29	2.17	1.46	6.1	7.63	0.38	B 3965-10	7
	PR 70	f		HK	2.88	±	0.07	2.49	2.31	48.9	0.82	0.87	B 3745-7	8
	PR 61	d	Diorite	HK	5.66	±	0.14	2.8	5.12	61.4	1.09	1.48	B 3763-7	8
4	SR 53	f	Andesite	HK	0.33	±	0.12	2.49	0.26	2.8	3.85	0.76	B 3756-9	9
					0.32	±	0.03		0.12	2.1	4.07		B 3751-4	
	SR 75	d	Bas. andesite	HK	0.37	±	0.02	3.21	0.38	14.4	0.77	2.36	B 3845-7	"
	SB 82	f	Basalt	MK	0.29	±	0.05	0.92	0.08	4.6	0.61	0.31	B 3761-5	10
	PS 31	b	Basalt	MK	0.38	±	0.04	0.72	0.08	7 7	0.35	0.01	B 3765-9	"
	SB 28	f	Andesite	MK	5.35	±	0.23	2.23	3.85	20.8	4.94	1 19	B 4260-3	"
														"
	SB 84	d	Andesite	MK	16.8	±	0.47	1.06	5.76	38.1	3.03	3.55	B 4191-6	"
	SB 83	d	Andesite	MK	16.8	±	0.39	1.43	7.77	78.7	0.71	1.54	B 3762-2	"
	SB 85	f	Andesite	MK	18.2	±	0.45	1.03	6.05	57.3	1.52	2.67	B 3777-3	"
	SB 27 B	d	Andesite	MK	19.6	±	0.58	1.61	10.25	35.3	6.36	1.77	B 3746-8	"
5	NL 46	b	Andesite	HK	1.19	±	0.03	2.23	0.85	48.4	0.3	1.21	B 3765-8	13
	NL 34	f	Absarokite	SH	18.2	±	0.44	1.07	6.32	61.3	1.35	2.59	B 3754-7	"
	NL 42	t	Basaltique	MK	19.7	±	0.48	0.96	6.14	62.7	1.24	3.60	B 4180-4	"
														"
	NL 37	d	Basalt	SH	37.4	±	0.9	2.3	28.25	67.4	4.58	2.56	B 4348-1	"
	NL 36	d	Andesite	MK	41 1	±	0.9	1.06	27.25	89.3	1.1	2.46	B 3743-5	"
	SU 49	d	Basalt	SH	52.1	±	1.2	2.53	43.13	93	1.09	2.58	B 4149-9	"
	NL 41	d	Andesite	HK	59.6	±	1.4	3.45	67.43	82.9	4.72	2.82	B 4244-2	"
	NL 40	d	Basalt	MK	62.5	±	1.4	1.33	27.27	86.8	1.4	2.69	B 3742-4	"

6) and southern (Lampung, 8) areas, and, conversely, low-K samples can be found all along the arc (table I). Cenozoic lavas from Sumatra are usually highly porphyritic, with plagioclase dominating over clinopyroxene, orthopyroxene and titanomagnetite phenocrysts. They display petrographic features often encountered in calc-alkaline lavas, e.g. strong and either normal or reverse zoning patterns, destabilised phenocrysts and other textural features usually associated with magma mixing processes [Sutanto, 1997].

Trace element characteristics

Cenozoic magmatic rocks of Sumatra usually contain low amounts of compatible transition elements, e.g. Cr, Co, Ni, and thus most of them do not represent primary melts from a peridotitic mantle wedge. Their incompatible element contents are moderate to high, and they generally display clearly enriched patterns on the mantle-normalised multielement plots shown in figure 4. High-K lavas among the Pliocene and Quaternary emissions (fig. 2) and high-K and shoshonitic lavas of Eocene, Oligocene and Miocene age in Padang and Lampung and also of Paleocene age in Natal (fig. 2) display larger enrichments in light rare earth elements (LREE) and large ion lithophile elements (LILE) compared to the medium-K and low-K ones. All individual sample patterns show strong negative niobium anomalies and somewhat lower negative Ti anomalies. These features are typical of "orogenic" (i.e. subduction- or collision-related) magmas.

Some individual spectras deserve special attention. First of all, samples from the 74 ka old Toba Tuff display significantly higher LREE and LILE contents compared to the

TABL. II. – *Datations isotopiques ^{40}K-^{40}Ar d'échantillons de Sumatra. Les âges avec des incertitudes pour un écart-type sont calculés selon les constantes de Steiger et Jäger [1977] prenant en compte la moyenne de deux analyses de l'argon 40 radiogénique (Ar*) les légendes des figures 1 et 2 pour la numérotation des régions d'échantillonnage et des coupes ; f : coulée ; d : dyke ; i : intrusion ; t : tuf ignimbritique. ; LK : laves calco-alcalines faiblement potassiques ; MK : laves calco-alcalines moyennement potassiques ; HK : laves calco-alcalines très potassiques ; SH : laves shoshonitiques.*

Center	Sample and outcrop		Type and parentage		Age (Ma)	±	error 1sigma	K_2O (wt%)	$^{40}Ar_R$ $10^{-7}cm^3.g^{-1}$	$^{40}Ar_R$ (%)	^{36}Ar $10^{-9}cm^3.g^{-1}$	LOI (wt%)	Analysis number	C.S. number
6	PY 76	d	Bas. andesite	HK	0.64	±	0.05	1.92	0.39	11.5	1.03	0.75	B 4052-9	15
	PLN 103	f	Bas. andesite	HK	1.35	±	0.1	1.63	0.71	11,0	1.93	5.41	B 3617-6	20
	MNJ 55	f	Andesite	MK	1.76	±	0.05	1.74	0.98	23.5	1.08	1.15	B 4394-8	17
	PY 82	f	Bas. andesite	MK	2.99	±	0.08	1.2	0.81	30.7	0.62	0.03	B 3591-5	15
	TP 32	f	Andesite	MK	14.3	±	0.34	2.26	10.49	63.8	2.01	1.27	B 4179-3	24
	PN 24	f	Basalt	HK	19.0	±	0.45	1 95	12.05	74.7	1.38	3.11	B 4181-5	23
	PN 22	f	Andesite	HK	19.1	±	0.45	3.58	22.19	78.7	2.03	0.28	B 4190-5	"
	PN 31	f	Andesite	MK	19.2	±	0.54	1.37	8.50	38.3	4.63	1.12	B 3616-5	"
	PN 26	f	Basalt	SH	23.7	±	0.55	2.34	17.99	77.4	1.78	0.72	B 3519-5	"
	TP 34	d	Andesite	MK	24.3	±	0.60	1 25	9.87	56.2	2.60	1.95	B 3585-8	24
	TP 33	d	Dacite	MK	25.5	±	0.59	1.20	9.92	74.	1.17	3.50	B 4261-4	"
	RDC 13	f	Basalt	LK	37.3	±	1	0.49	5.94	42.4	2.73	1.31	B 4189-4	21
	RDC 20	d	Basalt	SH	45.8	±	1.1	2.75	42.92	88.3	1.92		B 4322-3	"
	RDC 11	d	Gabbro	MK	62.9	±	1.5	1.41	29.11	66.6	4.94	2.07	B 4259-2	"
	RDC 13A2	f	Basalt	LK	63.1	±	1.5	0.55	11.39	58.3	2.65		B 4321-2	"
	RDC 13A1	f	Basalt	LK	63.7	±	1.5	0.58	12.1	61.9	2.53		B 4320-1	"
7	AM 165	f	Bas. andesite	MK	0.35	±	0.02	1.46	0.17	14.7	0.33	0.34	B 4036-5	27
					0.35	±	0.32		0 16	9.1	0.56		B 4025-6	
	LH 176	f	Bas. andesite	HK	0.81	±	0.06	1.85	0.48	12,0	1.19	0.34	B 4023-4	33
					0.81	±	0.05		0.48	14.5	0.97		B 4024-5	
	BS 129	d	Bas. andesite	MK	2.41	±	0.08	1.09	0.85	30.3	0.66	0.41	B 3626-8	32
	LH 178	d	Andesite	HK	2.91	±	0.09	2.11	1.98	32,0	1.43	2.16	B 4245-3	33
	CR 145	f	Bas. andesite	MK	4.23	±	0.15	1.3	0.52	25.5	0.51	1.21	B 3627-9	28
	LH 173	d	Basalt	LK	5.21	±	0.5	0.47	0.79	8.9	2.72	3.79	B 4216-5	33
	KP137	f	Bas. andesite	MK	5.40	±	0.14	1	1.76	42.1	0.82	1.39	B 4029-3	31
					5.47	±	0.14		1.76	42.1			B 4030-4	
	BN 111	f	Basalt	LK	6.45	±	0.2	0.29	1.74	48.1	0.63	0.76	B 3726-5	"
	MN 118	d	Rhyolite	MK	12.8	±	0.31	2.23	9.25	63.	1.84	1.87	B 4262-5	34
	MN 117	d	Bas. andesite	MK	12.8	±	0.38	0.91	3 77	35.1	2.36	1.60	B 3592-6	"
	MN 116	t	Andesite	MK	13.2	±	0.43	1 52	6.48	29.6	5.00	1.97	B 4188-3	"
	BSU 170	f	Andesite	MK	16.5	±	0.38	1.42	7.59	81.5	0.58	0.34	B 4395-9	29
8	R1 (rt)	t	Rhyolite	MK	0.99	±	0.08	1.98	0.63	10.5	1.83	1.6	B 4073-5	42
					1.21	±	0.18		0.77	5.7	4.31		B 4532-7	"
	(fds)				0.81	±	0.04	1.18	0.31	17.9	0.48		B 4096-7	"
					0.88	±	0.05		0.34	14.4	0.67		B 4533-8	"
	ms				0.59	±	0.14	4.45	0.86	3.5	7.92		B 4483-9	"
					0.81	±	0.14		1.22	5.1	7.72		B 4534-9	"
	KDG21	f	Andesite	MK	1.03	±	0.06	1.93	0.64	14.5	1.28	0.59	B 3723-2	39
	BK 26	f	Bas. andesite	HK	1.1	±	0.04	1.74	0.61	29.6	0.49	0.61	B 3725-4	35
	PC 16	f	Andesite	HK	4.93	±	0.13	2.1	3.34	49.8	1.14	0.46	B 3724-3	39
	SMK 37	d	Basalt	MK	10.9	±	0.43	0.43	1.52	26.2	1.45	2.81	B 4238-4	37
	PCE 9A	f	Dacite	HK	14.4	±	0.35	2.74	12.77	60.2	2.86	2.42	B 4370-3	"
	SMK 39	d	Basalt	LK	15.1	±	0.38	0.48	2.35	50.6	0.77	1.42	B 3595-9	"
	SMK 40	d	Andesite	MK	16.9	±	0.44	1 75	9.60	47.6	3.57	1.89	B 3594-8	"
	WS 5	d	Basalt	MK	17.1	±	0.44	1 11	6 13	48.2	2.23	0 13	B 3615-9	40
	TR 33	t	Rhyolite	MK	19.7	±	0.47	2.30	14.72	66.4	2.52	3.82	B 3629-2	41
	PCE 13	d	Shoshonite	SH	43.5	±	1	4.04	57.36	80.5	3.82	3.78	B 3620-2	39

others, which could reflect their anatectic origin already suspected from their high Sr isotopic ratios (0.710-0.714) [Gasparon and Varne, 1995]. Moreover, other acidic rocks such as the Quaternary Ranau Tuff in Lampung [Bellier *et al.*, 1999] and the Lasi granitoids in Padang area display very low heavy REE (HREE) and Y contents, similar to those of adakitic magmas presumably derived from the melting of subducting oceanic metabasalts [Defant and Drummond, 1990 ; Defant *et al.*, 1992 ; Maury *et al.*, 1996]. The Sr isotopic ratios (0.705 – 0.707) of the Ranau Tuffs [Gasparon and Varne, 1995], although higher than those of fresh oceanic basalts, are lower than those of the Toba Tuffs. However, the low HREE and Y contents of these rocks primarily reflects the occurrence of residual garnet in their magma source, whatever its continental (garnet-bearing metasediments) or oceanic (garnet amphibolite or eclogite) origin. Moreover, these silicic rocks do not show the relatively high MgO, Cr and Ni contents of typical adakitic magmas, which are thought to result from their interaction with the arc mantle wedge during their ascent. These chemical features could also reflect an anatectic origin through the melting of garnet-bearing metamorphic rocks from the lower Sumatran crust, an hypothesis already proposed by Nishimura *et al.* [1986].

^{40}K-^{40}Ar ages

About eighty new ^{40}K-^{40}Ar ages of Cenozoic magmatic rocks from Sumatra are presented in table II and in figure 2 where the temporal distribution (upper frame) and the geographical repartition (lower frame) are shown and can be easily related to each other. Ages have been obtained either

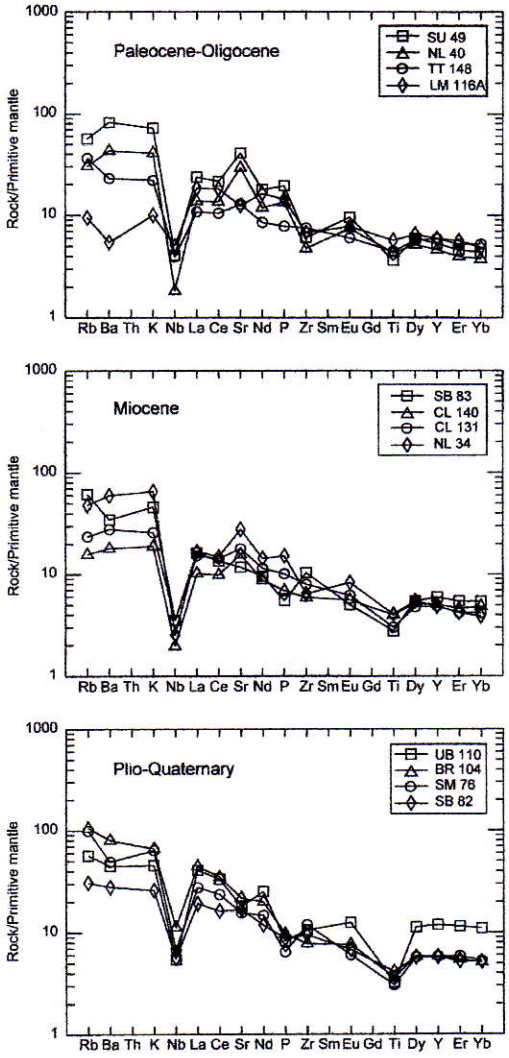

FIG. 4. – Incompatible multielement plots of selected Sumatra magmatic rocks normalised to the Primitive Mantle of Sun and McDonough [1989].
FIG. 4. – *Diagrammes multiélémentaires normalisés au manteau primitif de Sun et McDonough [1989] de roches magmatiques sélectionnées de Sumatra.*

on whole rocks or separated minerals, and range from 63.7 Ma to Recent, with two frequency peaks, the first one during the Middle Miocene (ca. 20 to 15 Ma) in seven sectors of investigation, that are along the coast and the second one during the Plio-Quaternary, at the rear of the Middle Miocene activity loci. Temporal patterns of this long activity will be detailed after.

Older activities have been documented earlier. Sutanto [1997] has obtained Mesozoic ages on minerals separated from ca. 20 Sumatra rocks, which are not presented in this paper. Among these magmatic rocks, a few volcanic ones have been dated to early Cretaceous (125-100 Ma, Hauterivian to Valanginian) or to late Cretaceous (90-75 Ma, Turonian to Campanian). On the other hand, three major plutonic events have been recognised based on mineral ages which give a complex ages pattern, comprising primary cooling ages and probable rejuvenated ages : early Jurassic (215-180 Ma), early Cretaceous (165-150 Ma) and late Cretaceous (125-110 Ma). These datings are consistent with previously published ages [McCourt *et al.*, 1996] for this subduction-related plutonism, mostly comprising I-type plutons formed by the northeasterly subduction beneath the continental margin of Sundaland [Barber, 2000].

DISCUSSION

Temporal patterns of magmatic activity

The data set shown in table I allows to discuss several features which have been schematically displayed in figure 2. In most tectonic reconstructions, subduction of the Indian Ocean beneath Sumatra is considered as effective since the early Eocene [Rangin *et al.*, 1990b ; Hall, 2002], based on the reported occurrence of subduction-related magmatism during that period [Hamilton, 1979 ; McCourt *et al.*, 1996]. Two main results arise from our data : i) calc-alkaline magmatic activity started at ca. 63 Ma during the Paleocene all along the island (areas 1, 5, 6, 8 in figure 2) and ii) that activity was probably permanent until Present at least in some areas.

The first conclusion is consistent with the ocean floor ages identified from magnetic anomalies [Müller *et al.*, 1997]. It is also in agreement with the probably more than 3500 km length of the subducted Indian Ocean slab below the western Sunda arc, according to tomographic data [Widiyantoro and van der Hilst, 1996]. However, the spatial distribution of magmatic activity seems to have increased in the early Miocene (20 Ma), a period during which this activity is documented in all the studied areas. This increase occurred prior to the development of the Sumatran Fault which was active (at least for its southern part) during the Pliocene, according to Pramumijoyo [1991]. The location of the Miocene volcanism seems controlled by the GSFZ and might be a consequence of its activity according to McCarthy and Elders [1997]. The closer location with respect to the trench of Paleocene-Miocene magmatic rocks compared to Plio-Quaternary ones (fig. 1) suggests that tectonic erosion [Von Huene and Lallemand, 1990] of the Sumatran margin was significant during the Cenozoic [Lallemand, 1999], and might have removed a few tens of kilometres from the Sumatran margin. As shown in figure 2, some periods of quiescence seem to appear in the eight investigated areas : between 50 and 25 Ma in Aceh, Toba, Sibolga and Bengkulu areas, whereas volcanic activity at 31.8 and 26.9 Ma is documented in Calang, an area adjacent to Aceh. However, these lacks could reflect possible sampling bias due to poor exposures. The lack of documented activity from 15 Ma until 6 Ma in Aceh, Calang, Toba, Sibolga, Natal and Padang might be representative, although it needs to be confirmed by further investigations.

Temporal geochemical patterns

The composition of subduction-related magmas is expected to reflect the respective contributions of their three main sources, i.e. the mantle wedge, the subducted crust and the upper crust on/through which they are emplaced [e.g., Kepezhinskas *et al.*, 1997]. Incomplete tapping by magmatic activity of the melts of metasomatised mantle wedge

peridotites might result into a temporal increase of incompatible elements in these magmatic rocks. Along-trench variations of the composition of the subducted slab, e.g. the thickness and detrital/pelagic character of its sediments, might cause along-arc compositional magmatic trends [e.g. White and Dupré, 1986]. However, the spatial and temporal distributions of K contents in Sumatran magmas do not reflect such trends (fig. 5), except that occurrences of K-rich calc-alkaline lavas seem to be more frequent during the Plio-Quaternary than before.

Selected incompatible trace element ratios have been plotted against time in figure 5, where data from Sumatra are compared to those of Java [from Bellon *et al.*, 1989 ; Soeria-Atmadja *et al.*, 1988, 1994]. The Cenozoic magmatism of Java differs from that of Sumatra by three main features, (i) it started later, at ca. 42 Ma, (ii) it was not emplaced through the Sundaland old continental crust, but through a Mesozoic accretionary prism which forms the southern half of the island, and finally (iii) the Indian Ocean crust subducting all along the Java Trench is rather homogeneous both in age (Cretaceous) and in the thickness of its pelagic sediment cover. Because of the second particularity, one can expect crustal contamination and anatexis to play a lesser role in the petrogenesis of the Java magmas compared

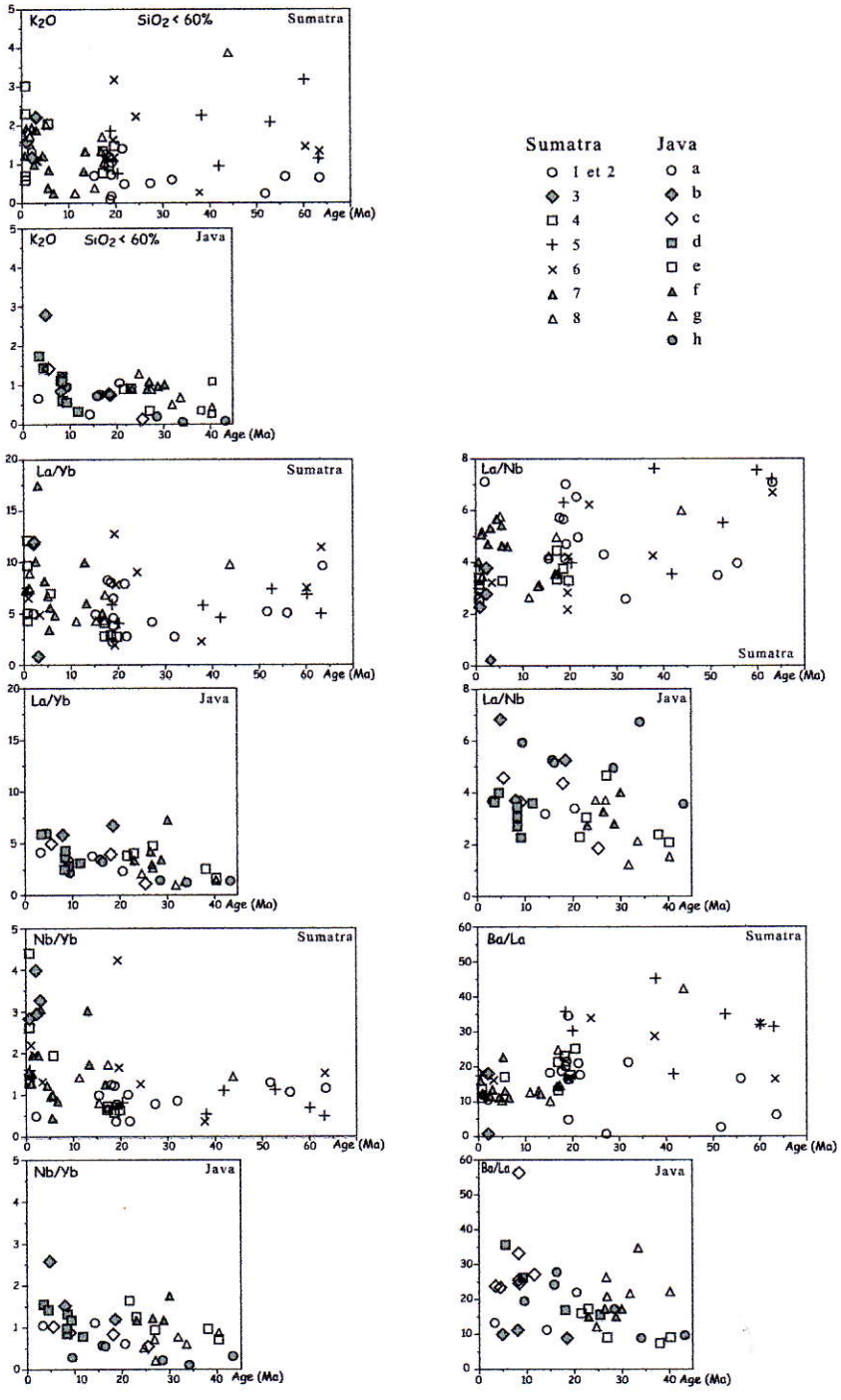

FIG. 5. – Temporal geochemical trends of Cenozoic magmatic rocks from Sumatra (this paper) and Java [ages according to Soeria-Atmadja *et al.*, 1994]. Numbers for Sumatra and letters for Java refer to locations in figure 1.

FIG. 5. – *Comparaison des évolutions géochimiques temporelles des roches magmatiques cénozoïques de Sumatra (cet article) et de Java [âges d'après Soeria-Atmadja* et al., *1994]. Les numéros pour Sumatra et les lettres pour Java renvoient aux localisations de la figure 1.*

to those from Sumatra. As a matter of fact, K_2O contents and ratios between elements of decreasing incompatibility (Ba/La, La/Yb, Nb/Yb) tend to increase with time in Java lavas, a feature which may be the result of incomplete tapping by magmatic activity of incompatible elements which are progressively accumulated into the mantle wedge through metasomatism. The temporal increase of La/Nb, a ratio between two elements of similar incompatibility but very different chemical properties (La is soluble and Nb insoluble in aqueous fluids), is also consistent with progressive accumulation of La in the Java mantle wedge metasomatised by hydrous fluids.

None of these features can be documented for Sumatra magmas based on figure 5 diagrams, which show a considerable scatter for the above-mentioned ratios. Such lacks of clear spatial and temporal geochemical patterns are often encountered in subduction-related magmas emplaced through continental crust. For instance, in the Andes, the complex petrogenesis of calc-alkaline magmas involves prolonged storage of the mantle-derived melts within the continental crust, leading to crustal contamination, assimilation coupled with fractional crystallisation (AFC) and crustal anatexis [Hildreth and Moorbath, 1988]. Other factors may have increased this complexity : for instance the changes of the thickness and composition of the subducted sedimentary pile northeastwards due to the contribution of detrital sediments (the Nicobar fan (inset, fig. 1)) from the Himalayas ; the subduction of the Wharton oceanic ridge beneath Central Sumatra ; and finally the tearing of the slab below the island [Widiyantoro and van der Hilst, 1996]. The relatively radiogenic Sr isotopic ratios of Sumatra lavas compared to other parts of the Sunda arc [Whitford, 1975 ; Gasparon and Varne, 1995] and the common occurrence of rhyolitic and presumably anatectic ignimbrites like the Quaternary Toba, Padang, Ranau and Lampung Tuffs suggest that the massive contribution of continental crust to the petrogenesis of Sumatran magmas overprinted the geochemical signatures of other processes.

CONCLUSION

The chronological data presented in this paper demonstrate that the magmatic activity of the Sunda arc started during the Paleocene rather than during the Eocene as reported by former authors. This conclusion is consistent with most of the SE Asia tectonic reconstructions [Hamilton, 1979 ; Rangin *et al.*, 1990a,b ; Hall, 1996, 2002]. There is no indication for any diachronism in the initiation of magmatism along the island. The near-trench position of Paleocene to Miocene magmatic units with respect to Plio-Quaternary volcanic centres suggests the occurrence of significant tectonic erosion of the Sundaland margin during the Cenozoic. Finally, the apparent lack of progressive spatial and temporal geochemical variations seems to reflect a particularly complex igneous petrogenesis, during which the Sundaland continental crust could play an important role through anatexis, contamination or AFC processes. Due to this scatter, the possible magmatic signature of major geodynamic features like the subduction of the Wharton ridge and/or the tearing of the downgoing slab cannot be identified anymore.

Acknowledgements. – This study has been done within the framework of French CNRS-INSU PICS 25 « Indonésie » and partly funded by the Université de Bretagne Occidentale SUCRI program « Asie du Sud-Est ». Sutanto's Ph.D. grant was funded by the World Bank. We thank Drs J. Malod, F. Hinschberger for scientific discussions, and O. Bellier, R. Montigny and an anonymous reviewer for their critical and constructive reviews.

References

BARBER A.J. (2000). – The origin of the Woyla terranes in Sumatra and the late Mesozoic evolution of the Sundaland margin. – *J. Asian Earth Sci.*, **18**, 713-738.

BELLIER O., BELLON H., SÉBRIER M., SUTANTO & MAURY R.C. (1999). – K/Ar age of the Ranau tuffs : implications for the Ranau caldera emplacement and the Great Sumatran Fault slip rate (Indonesia). – *Tectonophysics*, **312** (2/4), 347-359.

BELLIER O. & SÉBRIER M. (1994). – Relationship between tectonism and volcanism along the Great Sumatran Fault Zone deduced by SPOT image analyses. – *Tectonophysics*, **233**, 215-221.

BELLON H., QUOC BUU N., CHAUMONT J. &. PHILIPPET J.C. (1981). – Implantation ionique d'argon dans une cible support. Application au traçage isotopique de l'argon contenu dans les minéraux et les roches. – *C.R. Acad. Sci.*, Paris, **292**, 977-980.

BELLON H., SOERIA-ATMADJA R., MAURY R.C., POLVÉ M., PRINGGOPRAWIRO H. & PRIADI B. (1989). – Chronologie ^{40}K-^{40}Ar du volcanisme tertiaire de Java Central (Indonésie) : mise en évidence de deux épisodes distincts de magmatisme d'arc. – *C.R. Acad. Sci.*, Paris, **309**, II : 1971-1976.

CAMERON N.R., CLARKE M.C.G., ALDISS D.T., APSDEN J.A. & DJUNUDDIN A. (1980). – The geological evolution of northern Sumatra. – Indonesian Petrol Assoc., *Proceedings 9th Annual Convention*, Jakarta, **1**, 149-187.

CHAMOT-ROOKE N. & LE PICHON X. (1999). – GPS determined Sundaland motion with respect to Eurasia confirmed by earthquakes slip vectors at Sunda and Philippine trenches. – *Earth Planet. Sci. Lett.*, **173**, 439-455.

CHESNER C.A. & ROSE W.I. (1991). – Stratigraphy of the Toba Tuffs and the evolution of the Toba caldera complex, Sumatra, Indonesia. – *Bull. Volcanol.*, **53**, 343-356.

COTTEN J., LE DEZ A., BAU M., CAROFF M., MAURY R.C., DULSKI P., FOURCADE S., BOHN M. & BROUSSE R. (1995). – Origin of anomalous rare-earth element and yttrium enrichments in subaerially exposed basalts : evidence from French Polynesia. – *Chem. Geol*, **119**, 115-138.

DAVIES T.A., KIDD R.B. & RAMSAY A.T.S. (1995). – A time-slice approach to the history of Cenozoic sedimentation in the Indian Ocean. – *Sediment. Geol.*, **96**, 157-159.

DEFANT M.J. & DRUMMOND M.S. (1990). – Derivation of some modern arc magmas by melting of young subducted lithosphere. – *Nature*, **347**, 662-665.

DEFANT M.J., JACKSON T.E., DRUMMOND M.S., DE BOER J.Z., BELLON H., FEIGENSON M.D., MAURY R.C. & STEWART R.H. (1992). – The geochemistry of young volcanism throughout western Panama and southeastern Costa Rica : an overview. – *J. Geol. Soc. London*, **149**, 569-579.

DEFANT M.J., JACQUES D., MAURY R.C., DE BOER J. & JORON J.L. (1989). – Geochemistry and tectonic setting of the Luzon arc, Philippines. – *Geol. Soc. Amer. Bull.*, **101**, 663-672.

DEFANT M.J., MAURY R.C., JORON J.L., FEIGENSON M.D., LETERRIER J., BELLON H., JACQUES D. & RICHARD M. (1990). – The geochemistry and tectonic setting of the northern section of the Luzon arc, the Philippines and Taïwan. – *Tectonophysics*, **183**, 187-205.

DIAMENT M., HARJONO H., KARTA K., DEPLUS C., DAHRIN D., ZEN Jr M.T., GERARD M., LASSAL O., MARTIN A. & MALOD J. (1992). – Mentawai Fault zone of Sumatra : a new key to the geodynamics of western Indonesia. – *Geology*, **20**, 259-262.

GASPARON M. & VARNE R. (1995). – Sumatran granitoids and their relationship to Southeast Asian terranes. – *Tectonophysics*, **251**, 277-299.

HALL R. (1996). – Reconstructing Cenozoic Southeast Asia. *In* : R. HALL & D.J. BLUNDELL, Eds., Tectonic evolution of Southeast Asia. – *Geol. Soc. London Spec. Publ.*, **106**, 153-184.

HALL R. (2002). – Cenozoic geological and plate tectonic evolution of SE Asia and the SW Pacific : computer-based reconstructions, model and animations. – *J. Asian Earth Sci.*, **20**, 353-431.

HAMILTON W. (1979). – Tectonics of the Indonesian region. – *U.S. Geol. Surv. Prof. Paper*, **1078**, Washington, 345 p.

HILDRETH W. & MOORBATH S. (1988). – Crustal contribution to arc magmatism in the Andes of southern Chile. – *Contrib. Mineral. Petrol.*, **98**, 455-489.

HONTHAAS C., MAURY R.C., PRIADI B., BELLON H. & COTTEN J. (1999). – The Plio-Quaternary Ambon arc, eastern Indonesia. – *Tectonophysics*, **301** (3-4), 261-281.

HONTHAAS C., REHAULT J.P., MAURY R.C., BELLON H., HEMOND C., MALOD J.A., CORNÉE J.J., VILLENEUVE M., COTTEN J., BURHANUDDIN S., GUILLOU H. & ARNAUD N. (1998). – A Neogene back-arc origin for the Banda Sea basins : geochemical and geochronological constraints from the Banda ridges. – *Tectonophysics*, **298**, 297-317.

JUTEAU T. & MAURY R.C. (1999). – The oceanic crust : from accretion to mantle recycling. – Springer / Praxis ed., Chichester, U.K., 390 p.

KEPEZHINSKAS P., MCDERMOTT H.F., DEFANT M.J., HOCHSTAEDTER A., DRUMMOND M.S., HAWKESWORTH C., KOLOSKOV A., MAURY R.C. & BELLON H. (1997). – Trace element and Sr-Nd-Pb isotopic constraints on a three-component model of Kamchatka arc petrogenesis. – *Geochim. Cosmochim. Acta*, **61**, 577-600.

KOPP H., FLUEH E.R., KLAESCHEN D., BIALAS J. & REICHERT C. (2001). – Crustal structure of the central Sunda margin at the onset of oblique subduction. – *Geophys. J. Int.*, **147**, 449-474.

LALLEMAND S. (1999). – La subduction océanique. – Gordon and Breach Science Publishers, Paris, 194 p.

MAHOOD G.A. & DRAKE R.E (1982). – K-Ar dating young rhyolitic rocks : a case study of the Sierra la Primavera, Mexico. – *Geol. Soc. Amer. Bull.* **93**, 1232-1241.

MALOD J. & KEMAL M.R. (1996). – The Sumatra margin : oblique subduction and lateral displacement of the accretionary prism. *In* : R. HALL & D.J. BLUNDELL, Eds., Tectonic evolution of Southeast Asia. – *Geol. Soc. London Spec. Publ.*, **106**, 19-28.

MAURY R.C. (1984). – Les conséquences volcaniques de la subduction. – *Bull. Soc. géol. Fr.*, (7), **XXVI**, 489-500.

MAURY R.C., DEFANT M.J., BELLON H., JACQUES D., JORON F., MCDERMOTT F. & VIDAL P. (1998). – Temporal geochemical trends in northern Luzon arc lavas (Philippines) : implications on metasomatic processes in the island arc mantle. – *Bull. Soc. géol. Fr.*, **169**, 69-80.

MAURY R.C., SAJONA F.G., PUBELLIER M., BELLON H. & DEFANT M. (1996). – Fusion de la croûte océanique dans les zones de subduction / collision récentes : l'exemple de Mindanao (Philippines). – *Bull. Soc. géol. Fr.*, **167**, 579-595.

MCCARTHY A.J., JASIN B. & HAILE N.S. (2001). – Middle Jurassic radiolarian chert, Indarung, Padang District, and its implications for the tectonic evolution of western Sumatra, Indonesia. – *J. Asian Earth Sci*, **19**, 31-44.

MCCARTHY A.J. & ELDERS C.F. (1997). – Cenozoic deformation in Sumatra – the response to oblique subduction. *In* : A.J. FRASER, S.J. MATTHEWS & R.W. MURPHY, Eds., Petroleum geology of Southeast Asia. – *Geol. Soc. London Spec. Publ.*, **126**, 355-363.

MCCOURT W.J., CROW M.J., COBBING E.G. & AMIN T.C. (1996). – Mesozoic and Cenozoic plutonic evolution of SE Asia : evidence from Sumatra, Indonesia. *In* : R. HALL & D.J. BLUNDELL, Eds., Tectonic evolution of Southeast Asia. – *Geol. Soc. London Spec. Publ.*, **106**, 321-335.

MCDERMOTT F., DEFANT M.J., HAWKESWORTH C.J., MAURY R.C. & JORON J.L. (1993). – Isotope and trace element evidence for three component mixing in the genesis of the N. Luzon arc (Philippines). – *Contrib. Mineral. Petrol.*, **113**, 9-23.

MICHEL G.W., QUI YU Y., YUAN ZHU S., REIGBER C., BECKER M., REINHART E., SIMONS W., AMBROSIUS B., VIGNY C., CHAMOT-ROOKE N., LE PICHON X., MORGAN P. & MATHEUSSEN S. (2001). – Crustal motion and block behaviour in SE-Asia from GPS measurements. – *Earth Planet. Sci. Lett.*, **187**, 239-244.

MULLER R.D., ROEST W.R., ROYER J.-Y., GAHAGAN L.M. & SCLATER J.G. (1997) – Digital isochrons of the world's ocean floor. – *J. Geophys. Res.*, **102**, B2, 3211-3214.

NISHIMURA S., NISHIDA J., YOKOYAMA T. & HEHUWAT F. (1986). – Neo-tectonics of the strait of Sunda, Indonesia. – *J. SE. Asian Earth Sci.*, **1**, 81-91.

PECCERILLO A. & TAYLOR S.R. (1976). – Geochemistry of Eocene calc-alkaline volcanic rocks from the Kastamonu area, northern Turkey. – *Contrib. Mineral. Petrol.*, **58**, 63-81.

POLVÉ M., MAURY R.C., BELLON H., RANGIN C., PRIADI B., YUWONO S., JORON J.L. & SOERIA-ATMADJA R. (1997). – Magmatic evolution of Sulawesi (Indonesia) : constraints on the Cenozoic geodynamic history of the Sundaland active margin. – *Tectonophysics*, **272**, 69-92.

PRIADI B., POLVÉ M., MAURY R. C., BELLON H., SOERIA-ATMADJA R., JORON J.-L. & COTTEN J. (1994). – Tertiary and Quaternary magmatism in Central Sulawesi : chronological and petrological constraints. – *J. SE. Asian Earth Sci.*, **9**, 81-93.

PRAMUMIJOYO S. (1991). – Néotectonique et sismo-tectonique de la terminaison méridionale de la grande faille de Sumatra et du détroit de la Sonde (Indonésie). – Thèse de Doctorat, Univ. Paris Sud, 215 p.

PULUNGGONO A. & CAMERON N.R. (1984). – Sumatran microplates, their characteristics and their role in the evolution of Central and South Sumatra Basins. – Indonesian Petroleum Assoc., *Proceedings 13th Annual Convention*, Jakarta, **1**, 121-144.

RANGIN C., JOLIVET L., PUBELLIER M., AZÉMA J., BRIAIS A., CHOTIN P., FONTAINE H., HUCHON P., MAURY R.C., MULLER C., RAMPNOUX J.P., STEPHAN J.F. & TOURNON J. (1990a). – A simple model for the tectonic evolution of southeast Asia and Indonesia region for the past 43 m.y. – *Bull. Soc. géol. Fr.*, (8), **VI**, 889-905.

RANGIN C., PUBELLIER M., AZÉMA J., BRIAIS A., CHOTIN P., FONTAINE H., HUCHON P., JOLIVET L., MAURY R.C., MULLER C., RAMPNOUX J.P., STEPHAN J.F., TOURNON J., COTTEREAU N., DERCOURT J. & RICOU L.E. (1990b). – The quest for Tethys in the western Pacific. 8 paleogeodynamic maps for Cenozoic time. – *Bull. Soc. géol. Fr.*, (8), **VI**, 907-913.

SAJONA F.G., BELLON H., MAURY R.C., PUBELLIER M., QUEBRAL R.D., COTTEN J., BAYON F.E., PAGADO E. & PAMATIAN P. (1997). – Tertiary and Quaternary magmatism in Mindanao and Leyte (Philippines) : geochronology, geochemistry and tectonic setting. – *J. Asian Earth Sci.*, **15**, 121-153.

SAJONA F.G., BELLON H., MAURY R.C., PUBELLIER M., COTTEN J. & RANGIN C. (1994). – Magmatic response to abrupt changes in geodynamic settings : Pliocene-Quaternary calc-alkaline and Nb-enriched lavas from Mindanao (Philippines). – *Tectonophysics*, **237**, 47-72.

SAJONA F., MAURY R.C., BELLON H., COTTEN J., DEFANT M.J. & PUBELLIER M. (1993). – Initiation of subduction and the generation of slab melts in western and eastern Mindanao, Philippines. – *Geology*, **21**, 1007-1010.

SIMANDJUNTAK T.O. & BARBER A.J. (1996). – Contrasting tectonic styles in the Neogene orogenic belts of Indonesia. *In* : R. HALL & D.J. BLUNDELL, Eds., Tectonic evolution of southeast Asia. – *Geol. Soc. London Spec. Publ.*, **106**, 185-201.

SOERIA-ATMADJA R., MAURY R.C., BELLON H., PRINGGOPRAWIRO H., POLVÉ M. & PRIADI B. (1994). – Tertiary magmatic belts in Java. – *J. SE Asian Earth Sci.*, **9**, 13-27.

SOERIA-ATMADJA R., MAURY R.C., BELLON H., YUWONO Y.S. & COTTEN J. (1988). – Remarques sur la répartition du volcanisme potassique quaternaire de Java (Indonésie). – *C.R. Acad. Sci.*, Paris, **307**, II, 635-641.

STEIGER R. H. & JÄGER E. (1977). – Subcommission on geochronology : Convention on the use of decay constants in geo- and cosmochronology. – *Earth Planet. Sci. Lett.*, **36**, 359-362.

SUN S.S. & MCDONOUGH W.F. (1989). – Chemical and isotopic systematics of oceanic basalts : implications for mantle composition and processes. *In* : A.D. SAUNDERS & M.J. NORRY, Eds, Magmatism in the ocean basin. – *Geol. Soc. London Spec. Publ.*, **42**, 313-345.

SUTANTO (1997). – Evolution temporelle du magmatisme d'arc insulaire : géochronologie, pétrologie et géochimie des magmatismes mésozoïques et cénozoïques de Sumatra (Indonésie). – Thèse de Doctorat, Univ. Bretagne Occidentale, Brest, 247 p.

TREGONING P., BRUNNER F.K., BOCK Y., PPUNTODEWO S.S.O., MCCAFFREY R., GENRICH J., CALAIS E., RAIS J. & SUBARYA C. (1994). – First geodetic measurement of convergence across the Java Trench. – *Geophys. Res. Lett.*, **21**, 2135-2138.

VON HUENE R. & LALLEMAND S. (1990). – Tectonic erosion along convergent margins. – *Geol. Soc. Amer. Bull.*, **102**, 704-720.

WHITE W.M. & DUPRÉ B. (1986). – Sediment subduction and magma genesis in the Lesser Antilles : isotopic and trace element constraints. – *J. Geophys. Res.*, **91**, 5927-5941.

WHITFORD D.J. (1975). – Strontium isotopic studies of the volcanic rocks of the Sunda arc, Indonesia and their petrogenetic implications. – *Geochim. Cosmochim. Acta*, **39**, 1287-1302.

WIDIYANTORO S. & VAN DER HILST R. (1996). – Structure and evolution of lithospheric slab beneath the Sunda Arc, Indonesia. – *Science*, **271**, 1566-1570.